Tunable fluid-loaded free-electron laser in the low-electron-energy and long-wavelength extreme

R. Drori and E. Jerby*
Department of Electrical Engineering, Physical Electronics, Faculty of Engineering, Tel Aviv University, Ramat Aviv 69978, Israel
(Received 1 October 1998)

A tunable fluid-loaded free-electron laser (FEL) oscillator is demonstrated. This FEL-type experiment employs low-energy electrons, down to 0.4 keV. Therefore, it interacts with extremely long radio waves, in the VHF range ($\lambda > 1$ m). The device consists of a folded-foil planar wiggler ($\lambda_W = 4$ cm), and a double-stripline cavity. The variable dielectric loading is implemented by distilled water in glass pipes situated on both sides of the stripline structure. Coherent oscillations are observed at the fundamental cavity mode, around 270 MHz. By varying the fluid dielectric loading, the operating frequency is tuned in a range of 10 MHz. This paper presents (a) the effect of a variable dielectric loading on the FEL tunability in general, and (b) an extremely low-electron-energy and long radiation wavelength, in the lowest end of the known FEL operating spectrum. [S1063-651X(99)03703-4]

PACS number(s): 52.75.Ms, 33.20.Bx, 41.60.Cr, 84.40.Az

I. INTRODUCTION

In free-electron lasers (FELs) [1,2], the electron beam undulates along a periodic, transversely polarized magnetic field, known as the wiggler field, and interacts with an electromagnetic wave which propagates in a hollow waveguide or in free space. The synchronism condition of the FEL interaction is given for a tenuous, mono-energetic electron beam, by

$$\omega \cong \frac{\omega_W}{1 - v_{ez}/v_{\mathrm{ph}}}, \tag{1}$$

where ω and v_{ph} are the em-wave angular frequency and phase velocity, respectively, and v_{ez} is the average axial velocity of the electrons. Their wiggling frequency is defined as $\omega_W = v_{ez} k_W$, where $k_W = 2\pi/\lambda_W$ is the wiggler periodicity. Equation (1) describes the fundamental tuning relation between the three FEL elements; the electron beam, the em wave, and the wiggler. The simplified tuning relation (1) neglects electron energy spread and space-charge effects [3].

The Doppler up shift, a fundamental operating principle of the short-wavelength FEL, is presented in the denominator of Eq. (1). For FELs operating with relativistic electron beams in free space ($v_{ez} \to c$, $v_{\mathrm{ph}} = c$), the denominator tends to be infinitesimally small, hence, the Doppler up shift is large ($\omega \gg \omega_W$) and the radiation wavelength is much shorter than the wiggler period ($\lambda \ll \lambda_W$). Relativistic FELs operate in the infrared [4], visible [5], and ultraviolet [6] regimes.

Ubitrons [7] and free-electron masers (FEMs) [8] form another type of FEL devices. These microwave tubes operate in the centimeter- and millimeter-wave regimes with mildly relativistic electron beams. FEMs employ, usually, hollow metallic waveguides, for which $v_{\mathrm{ph}} > c$. This reduces further the Doppler-shift term in Eq. (1). Consequently, FEMs operate typically at $\lambda \leqslant \lambda_W$.

The ubitron-FEM often includes also an axial magnetic field B_0, to guide the electron beam. The electron axial velocity v_{ez} in Eq. (1) is then related approximately to the magnetic field parameters and the electron energy by [1]

$$\frac{V_{ez}^2}{c^2}\left[1 + \frac{\Omega_W^2(\Omega_0^2 + \omega_W^2)}{2(\Omega_0^2 - \omega_W^2)^2}\right] \cong 1 - \frac{1}{\gamma^2}, \tag{2}$$

using the definition $\Omega_{W,0} = eB_{W,0}/\gamma m$, where e and m are the electron charge and mass, respectively, and γ is the relativistic factor. The characteristic solutions of Eq. (2) are classified as Group I and Group II solutions, for $\Omega_0 < \omega_W$ and $\Omega_0 > \omega_W$, respectively [Eq. (2) is not valid near resonance, where $\Omega_0 \sim \omega_W$]. The axial magnetic field may excite a cyclotron interaction in addition to the ubitron-FEL interaction, as observed in Ref. [9].

Our previous work [9–11] extended the operating range of the known FEL-type interaction toward long radio wavelengths (>1 m), and toward extremely low electron energies (<1 keV). These FEL-type devices employ a TEM mode in transmission lines in which $v_{\mathrm{ph}} = c$, as in the short-wavelength free-space FELs. The Doppler shift, however, almost vanishes because of the slow electron beam ($v_{ez} \approx 0.05c$), and the tuning condition (1) is reduced to $\omega \approx \omega_W$. The em wavelength, in the VHF radio band, is much longer than the wiggler period ($\lambda \gg \lambda_W$). The operating frequency and electron energy in these experiments [9–11] are much lower than those of any known FEM experiment [12]. This new operating regime differs, substantially, from that of the mature FEL and FEM types, hence, the acronym FER (R for radio) was proposed to define it [11]. The main features of the FEL, FEM, and FER types are compared in Table I.

The wide spectrum of FEL experiments worldwide [2,12] is presented in Fig. 1, which maps the operating wavelengths of FELs vs their electron energies. Figure 1 shows also a representative solution of the tuning Eq. (1) for $\lambda_W = 4$ cm (assuming $v_{ez} \cong c\sqrt{1 - \gamma^{-2}}$ and $v_{\mathrm{ph}} = c$). This analytical curve coincides with the general tendency of the FEL experiments, despite their variety of wiggler periods and strength.

*FAX: +972 3 6423508. Electronic address: jerby@eng.tau.ac.il

TABLE I. Features of FERs vs features of typical FEMs and FELs.

	FEL	FEM	FER
e energy	highly relativistic	mildly relativistic	extremely low
em guide	free space	hollow waveguide	transmission line
wavelength	microns	millimeters	meters
λ vs λ_w	$\lambda \ll \lambda_w$	$\lambda \leqslant \lambda_w$	$\lambda \gg \lambda_w$

Our FER experiments [9–11] mark the lowest extreme of the worldwide FEL operating-spectrum map. These FER experiments have yielded 0.8 GHz at 1 keV [9], and 0.28 GHz at 0.75 keV [11]. The latter radiates also at higher longitudinal modes (0.56 GHz at 2.5 keV, and 0.85 GHz at 5.7 keV).

The FEL and FEM types mentioned above operate in free space or in hollow (uniform) waveguides, hence with fast em waves, $v_{\rm ph} \geqslant c$. Slow-wave FELs with magnetic wigglers (i.e., excluding Cherenkov devices) have been studied in various schemes, in structures of solid dielectrics [13], periodic waveguides [14], and gas-loaded FELs [15]. The interaction with slow-wave ($v_{\rm ph} < c$) increases the FEL Doppler shift, as results from Eq. (1).

The fluid loading of microwave tubes was proposed first in Ref. [16] as an inherent component of the electron-wave interaction. A fluid-loaded-FER version of this concept is presented in this paper. This FER experiment demonstrates the principle of FEL tunability by a variable dielectric loading of the FEL interaction region. In view of Eq. (1), $v_{\rm ph}$ is varied by an external means in this experiment. This tuning method is applicable by other means also to shorter wavelength FELs.

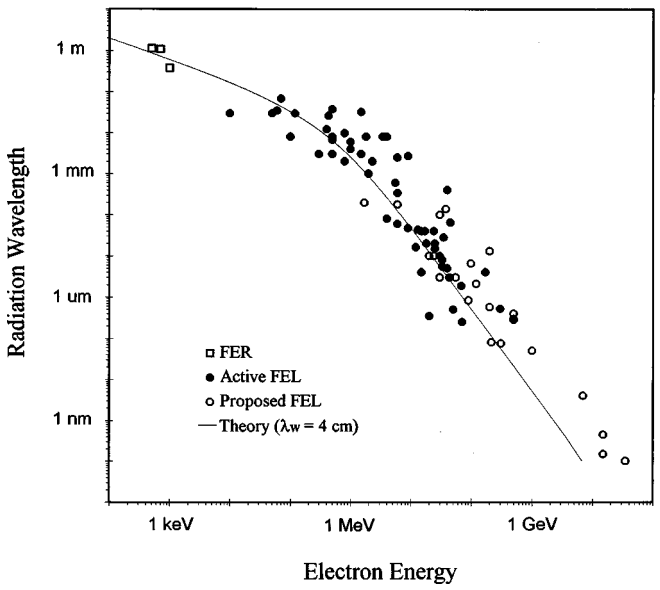

FIG. 1. The spectral diversity of FEL experiments worldwide. The dots and circles show tuning parameters of performed and proposed FEL experiments, respectively [2,12]. The squares represent previous FER experiments in the long-wavelength limit [9–11]. The solid curve shows the analytic FEL tuning relation (1) for $\lambda_W = 44$ cm (weak wiggler).

II. EXPERIMENTAL SETUP

A principle scheme of the fluid-loaded FEL device is shown in Fig. 2. The interaction region includes four glass pipes situated on both sides of two metallic striplines along a rectangular waveguide. The metallic striplines support a quasi-TEM mode. They suppress any axial electric field component (E_z) and eliminate the possibility for a Cherenkov interaction in this device. These metallic striplines also protect the glass pipes from the electrons, hence prevent their electrical charging.

The effective dielectric coefficient of this transmission line in its quasi-TEM fundamental mode [i.e., $\epsilon_{\rm eff} = (c/v_{\rm ph})^2$] is determined by the amount of distilled water in the pipes. The FEL tuning Eq. (1) is given for this scheme by

$$\omega \cong \frac{\omega_W}{1 \mp \sqrt{\epsilon_{\rm eff}} v_{ez}/c}, \tag{3}$$

where $\epsilon_{\rm eff}$, and consequently ω, are controlled externally. The $\mp$ sign indicates, explicitly, the forward $(-)$ and backward $(+)$ wave interactions.

Two mirrors with holes at both ends of the transmission line form a 0.53 m long cavity. The resonance frequency of the cold cavity (i.e., without an electron beam) is measured by a vector network analyzer (HP8714B) in a *one-port* scattering analysis mode. A probing frequency-swept signal is injected into the cavity, while its reflection coefficient is measured. A minimum in the reflection trace indicates a resonance frequency. Figure 3(a) shows, for instance, power reflection measurements of the cold cavity resonances in two extreme levels of distilled water in the glass pipes. The minima in the two reflection traces show the corresponding resonance frequencies, 266 MHz and 276 MHz, for full and empty glass pipes, respectively. The fundamental resonance frequency of the cavity without the glass pipes at all is 285 MHz.

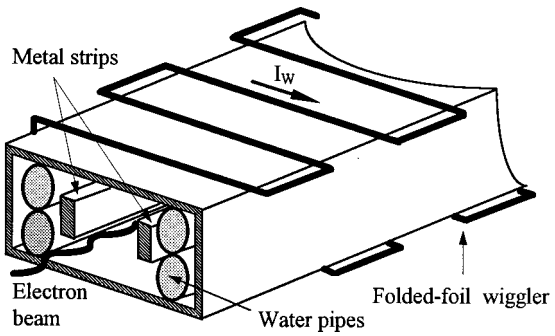

FIG. 2. A principle scheme of the fluid-loaded FEL-type experimental device.

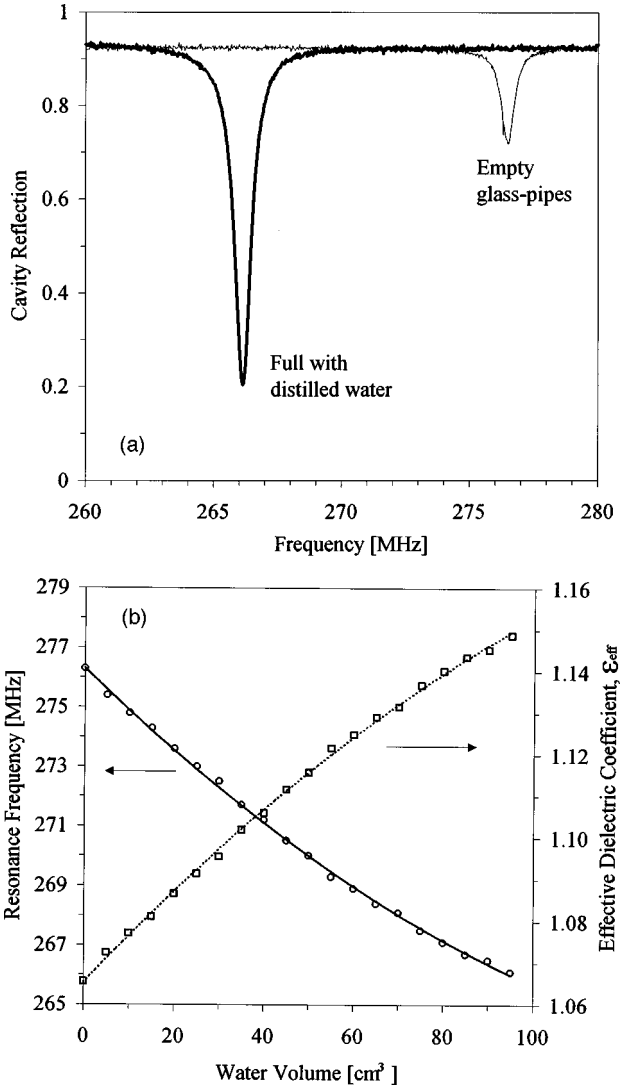

FIG. 3. The (cold) cavity resonance-frequency measurements: (a) Power reflection traces for full and empty glass pipes. (b) Resonance-frequency tunability in a range of water loads, and the corresponding effective dielectric coefficient ϵ_{eff} [from Eq. (4)].

The effective dielectric coefficient ϵ_{eff} of the transmission line, operating in the fundamental quasi-TEM mode, is deduced from the variation in the resonance frequency caused by the water loading, i.e.,

$$\epsilon_{\text{eff}}(q)=\left(\frac{f_{R0}}{f_R(q)}\right)^2, \tag{4}$$

where q is the quantity of water in the pipes, and f_{R0} and $f_R(q)$ are the cavity resonance frequencies without the glass pipes, and with pipes filled with the actual amount of water, respectively, (i.e., $f_{R0}=285\,\text{MHz}$). Results of resonance-frequency measurements in a range of water loads, and the corresponding dielectric coefficient ϵ_{eff} (4), are presented in Fig. 3(b). A range of $\epsilon_{\text{eff}}=1.06$ to 1.15 is obtained by varying the water loading between empty and full pipes, respectively.

A low-energy electron beam (<1 keV) emitted from a planar thermionic cathode is confined by an axial magnetic field [9]. The collector current is measured by a 50 Ω resistor. A five-layer coaxially fed folded foil forms a planar wiggler [17] with $\lambda_W=4$ cm. The wiggler is tapered at both ends for adiabatic entrance and exit of the electron beam. This experimental setup operates in a single-pulse mode.

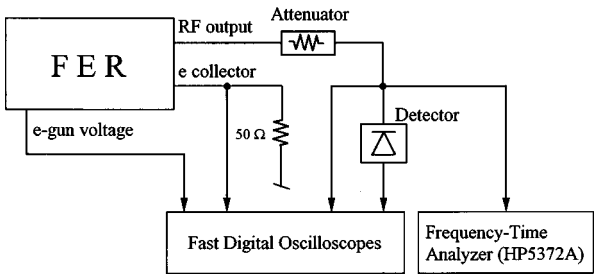

FIG. 4. The diagnostic setup of the FER experiment.

The diagnostic setup is illustrated in Fig. 4. The em wave evolved in the FER cavity is sampled by an rf probe located in the middle of the cavity. The sampled signal is attenuated and split for power and spectral measurements. The signal is detected by a calibrated crystal detector. The FER output signal is observed also directly (without any detection) by a fast digital oscilloscope at a sampling rate of 1 G samples/s [11]. The frequency variation along the pulse is measured by a frequency-time interval analyzer (HP5372A).

III. EXPERIMENTAL RESULTS

The operating parameters of the fluid-loaded FER experiment are listed in Table II. According to these parameters, the orbits of the electrons are characterized as Group II orbits ($\Omega_0/2\pi\approx 4\,\text{GHz}$, $\omega_W/2\pi\approx 0.4\,\text{GHz}$). The performance of this device and its tunability features in various loading conditions are presented in this section.

A typical FER pulse is shown in Figs. 5(a)–5(d). The effective dielectric coefficient in this example is $\epsilon_{\text{eff}}=1.11$. The detected output signal and the corresponding electron-gun voltage pulse are shown in Figs. 5(a) and 5(b), respectively. The actual frequency during the pulse, measured by the frequency-time interval analyzer (HP5372A), is presented in Fig. 5(c). This reveals the frequency-modulation

TABLE II. Experimental parameters

Electron beam		
Energy	0.4–1	[keV]
Current	~0.2	[A]
Pulse width	~2	[ms]
Magnetic field		
Wiggler period	4.0	[cm]
Wiggler strength	0.2–0.4	[kG]
Uniform solenoid	1–2	[kG]
Waveguide		
Rectangular tube	1.87×0.87	[inch^2]
Stripline width	1.9	[mm]
Distance between striplines	10.2	[mm]
Cavity length	52.6	[cm]
Effective dielectric range	1.06–1.15	
rf output		
Frequency tunability	266–276	[MHz]
Detected output power	~3	[W]

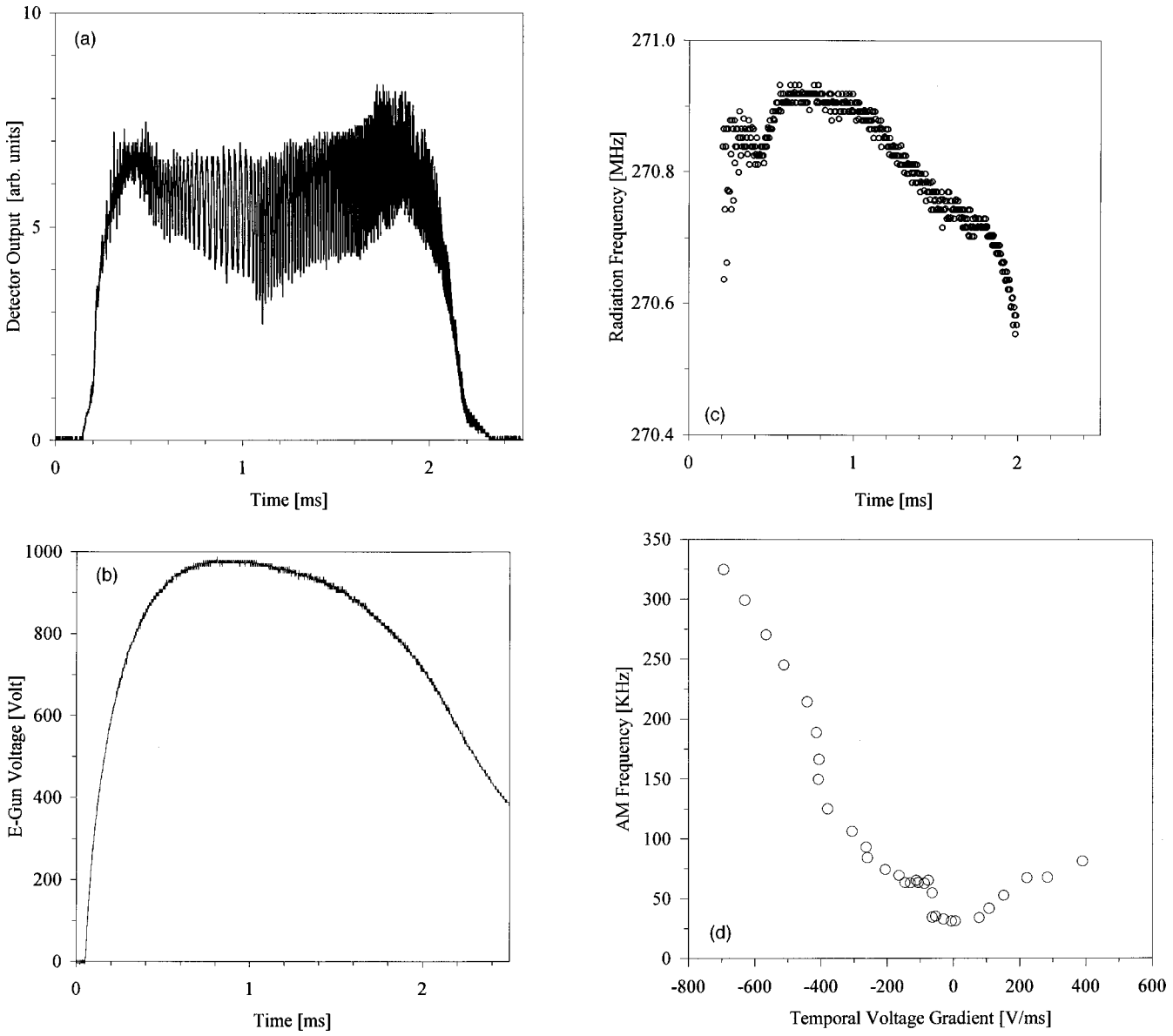

FIG. 5. A typical FER output signal with a medium dielectric loading, $\epsilon_{\text{eff}}=1.11$: (a) The detected FER output signal. (b) The electron-gun voltage pulse. (c) The actual FER frequency during the pulse (HP5372A measurements). (d) The amplitude modulation (AM) frequency with respect to the voltage gradient.

(FM) effect and shows that the sweep of the FER output frequency tends to follow the electron-gun-voltage variation [Fig. 5(b)]. It is noted that radiation frequencies for increasing voltages are slightly higher than those measured for the same decreasing voltages. In addition, amplitude fluctuations are clearly seen in the trace of the detected output power in Fig. 5(a). The frequency of this amplitude modulation (AM), counted with respect to the instantaneous voltage gradient, is presented in Fig. 5(d). For each amplitude fluctuation period (ΔT), the instantaneous frequency ($1/\Delta T$) and the corresponding temporal voltage gradient ($\Delta V/\Delta T$) are computed. Both FM and AM frequency measurements [Figs. 5(c) and 5(d), respectively] show similar ranges of FER frequency variations ($\sim$0.3 MHz) during the voltage pulse. (This may hint that both effects are associated, maybe through the interrelations between the FER phase shift and the varying electron energy, and the cavity resonance.) These effects require further theoretical and experimental studies.

Increasing the fluid loading reduces both the FER oscillation frequency and the operating voltage. Figure 6 shows the rf detector output, the *e*-gun voltage, and the rf frequency, for $\epsilon_{\text{eff}}=1.15$. The oscillations are excited in the leading and trailing edges of the voltage pulse, from 420 to 640 V. The rf frequency shift during the pulse (measured by the HP5372A) follows the voltage sweep.

The tunability of the fluid-loaded FER is shown in Fig. 7, as results in many runs with different dielectric loads. The inverse dependence of the FER oscillation frequency on the dielectric loading is almost linear in this range. The electron axial velocity, computed by Eq. (2) for data measured in different experimental runs, is shown in Fig. 8 [i.e., the actual wiggler and solenoid fields and the electron energy in each run are substituted to Eq. (2) to find v_{ez}]. Each run is represented by the minimal and maximal electron velocities in which radiation is observed. The experimental results for v_{ez} are larger than those predicted analytically by Eq. (3) for

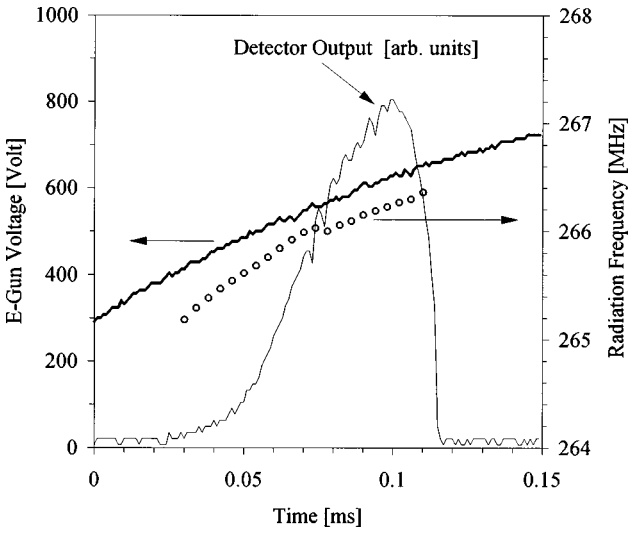

FIG. 6. A typical FER output with a full dielectric loading, $\epsilon_{\text{eff}}=1.15$, at low voltage ($\geqslant$420 V). The FER output-signal frequency (○) sweeps with the *e*-gun voltage increase.

a backward-wave interaction. [Note that a slight space-charge detuning [3] added to Eq. (3) eliminates this deviation.] The energy spread acceptance observed in these experiments is considerably wide, and the relative energy detuning exceeds 10%. However, the tendency of the axial velocity to decrease as the dielectric loading increases is similar in both experimental and analytical lines in Fig. 8.

The FER electronic efficiency (i.e., the ratio between the coupled output signal and the electron-beam power) is shown in Fig. 9. The efficiency tends to increase with the dielectric loading, and it exceeds an average of ~2%. This result can be improved by a stable operation and an optimal coupling in a future experiment.

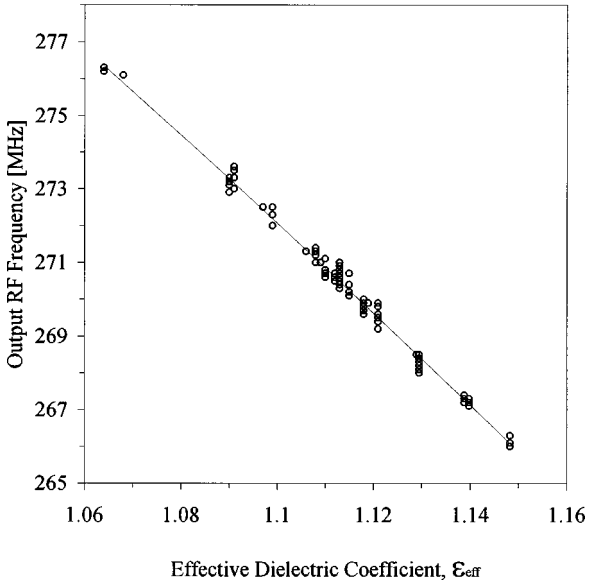

FIG. 7. The fluid-loaded FER tunability. The circles indicate center-frequency measurements in many pulses, in different dielectric loading conditions.

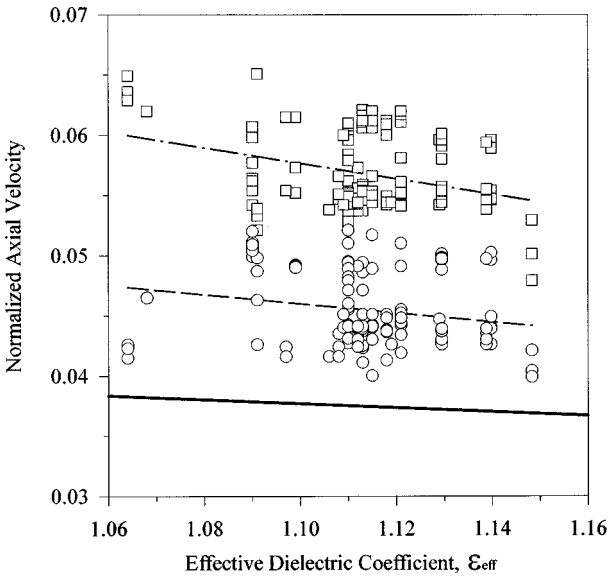

FIG. 8. Maximal (□) and minimal (○) normalized axial velocities (v_{ez}/c) in many FER pulses. These are computed by Eq. (2) for actual experimental data logged in many runs. (The dashed lines are their linear fits.) The solid curve shows for comparison the result of the analytic tuning relation (3) for a backward wave (the forward wave interaction results in a smaller axial velocity).

IV. CONCLUSIONS

The FER devices presented here and in Refs. [9–11] obey the basic physical rules of the mature FEL types, though they operate at extremely low voltages and long wavelengths at the lowest end of the FEL operating spectrum (266 MHz at 420 V).

A method of FEL tuning by a variable-dielectric loading is demonstrated successfully. This concept could be relevant, in general, as a method to tune FELs in both oscillator and amplifier schemes. The variable dielectric, demonstrated here by the fluid loading, can be implemented by solid materials as well, either by a variable geometry or by a ferroelectric material. Compared to the known method of FEL tuning by electron-energy variation, the controlled dielectric

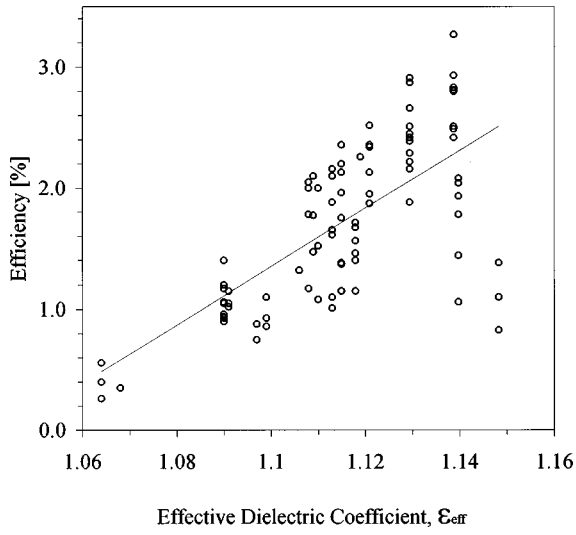

FIG. 9. The FER output-coupling efficiency with respect to ϵ_{eff}.

loading alleviates the need to change the accelerator and electron-optics settings.

For scientific purposes, the FERs can be used as table-top experiments to study fundamental FEL physics (even in small laboratories). For instance, the electron bunching structure could be easily observed, as suggested in Ref. [18], or, efficiency enhancement could be studied by tapering the fluid dielectric loading along the tube (simply by tilting it). The low-cost FER can be used even for educational purposes to demonstrate FEL operation.

For practical purposes, a high-power FER version with enhanced efficiency may add another range of applications to the diverse FEL family. Practical applications, in the UHF and VHF bands, include a wide range of industrial processes, radio communication, radar, rf accelerators, and plasma processing. The FER tunability, demonstrated in this paper, could be a useful feature in these applications. As compared to existing rf sources (klystrons, for instance), the FER introduces the known advantages of *fast-wave* devices. The FER concept is believed, therefore, to be a useful extension of the FEL family in both scientific and practical aspects.

ACKNOWLEDGMENTS

This work was supported in part by the Israeli Academy of Sciences and Humanities, and by the Israeli Ministry of Energy and the Belfer Center for Energy Research.

[1] H. P. Freund and T. M. Antonsen, Jr., *Principles of Free-electron Lasers* (Chapman and Hall, London, 1992), and references therein.

[2] W. B. Colson, Nucl. Instrum. Methods Phys. Res. A **393**, 6 (1997).

[3] E. Jerby and A. Gover, IEEE J. Quantum Electron. **21**, 1041 (1985).

[4] L. R. Elias, W. M. Fairbank, J. M. J. Madey, H. A. Schwettman, and T. I. Smith, Phys. Rev. Lett. **36**, 717 (1976).

[5] M. Billardon, P. Elleaume, J. M. Ortega, C. Bazin, M. Bergher, M. Velghe, Y. Petroff, D. A. G. Deacon, K. E. Robinson, and J. M. J. Madey, Phys. Rev. Lett. **51**, 1652 (1983).

[6] G. N. Kulipanov, V. N. Litvinenko, I. V. Pinaev, V. M. Popik, A. N. Skrinsky, A. S. Sokolov, and A. N. Vinokurov, Nucl. Instrum. Methods Phys. Res. A **296**, 1 (1990).

[7] R. M. Phillips, IRE Trans. Electron Devices **7**, 231 (1960); Nucl. Instrum. Methods Phys. Res. A **272**, 1 (1988).

[8] T. J. Orzechowski, B. R. Anderson, J. C. Clark, W. M. Fawley, A. C. Paul, D. Prosnitz, E. T. Scharlemann, S. M. Yarema, D. B. Hopkins, A. M. Sessler, and J. S. Wurtele, Phys. Rev. Lett. **57**, 2172 (1986).

[9] R. Drori, E. Jerby, and A. Shahadi, Nucl. Instrum. Methods Phys. Res. A **358**, 151 (1995).

[10] R. Drori, E. Jerby, A. Shahadi, M. Einat, and M. Sheinin, Nucl. Instrum. Methods Phys. Res. A **375**, 186 (1996).

[11] R. Drori and E. Jerby, Nucl. Instrum. Methods Phys. Res. A **393**, 284 (1997).

[12] H. P. Freund and V. L. Granatstein, Nucl. Instrum. Methods Phys. Res. A **393**, 9 (1997).

[13] M. Einat and E. Jerby, Phys. Rev. E **56**, 5996 (1997).

[14] E. Jerby, Phys. Rev. A **44**, 703 (1991).

[15] J. Feinstein, A. S. Fisher, M. B. Reid, A. Ho, H. D. Dulman, and R. H. Pantel, Phys. Rev. Lett. **60**, 18 (1988).

[16] E. Jerby, IL Patent App. No. 114745, PCT/IL96/00054 (26 July 1995).

[17] A. Sneh and E. Jerby, Nucl. Instrum. Methods Phys. Res. A **285**, 294 (1989).

[18] K. J. Kim (unpublished).